# Hydrodynamic instabilities and Soret effect in an aqueous electrolyte

J. Colombani, H. Dez, J. Bert, and J. Dupuy-Philon
*Département de Physique des Matériaux, CNRS Unité Mixte de Recherche 5586, Université Claude Bernard Lyon 1, 43 Boulevard du 11 Novembre, F-69622 Lyon-Villeurbanne, France*

(Received 29 July 1997; revised manuscript received 9 March 1998)

In order to gain reliable thermal diffusion measurements, which enable a microscopic interpretation of this effect, we have studied the hydrodynamical stability of a confined (LiCl, $9.7H_2O$) mixture submitted to both temperature and concentration gradients. A comparison with Rayleigh-Bénard experiments in binary mixtures has been undertaken that emphasizes the influence of the confinement. This study has permitted one to carry out interdiffusion and Soret coefficient measurements of the liquid, free from any convective disturbance. Opposite to initial predictions, the Soret coefficient appears to be largely negative and these results weaken some assumptions about the origin of the sign inversion of the effect, which is still questionable.
[S1063-651X(98)09209-5]

PACS number(s): 47.20.Bp, 66.10.Cb, 42.40.Kw

## I. INTRODUCTION

Thermal diffusion in liquids (a diffusion of matter caused by a temperature gradient), the so-called Soret effect, has aroused considerable interest for several years, due to the progress of the molecular dynamics simulations, which now partially recover experimental results [1], to the appearance of new measurement techniques, such as thermal diffusion forced Rayleigh scattering [2] or fiber-optic spectroscopy [3], and to the richness of the hydrodynamical behavior of this nonequilibrium pattern forming system, deriving from the interplay between heat and mass transport [4].

Nevertheless, experimental determination of the Soret coefficient $S_T$ of liquids faces many difficulties, stemming from the facility with which convection arises in such systems. Though appreciable advances in our understanding of this nonlinearly behaving system allow the use of stability criteria for pure Soret effect experiments, reproducibility of the thermal diffusion coefficient measurement of one system with various experimental techniques is still difficult to gain. This problem is illustrated by the experimental review of Legros *et al.* on methanol-benzene [5] and by the recent discussion about the ethanol-water and *n*-hexane-toluene mixtures [6–9] and confirmed by the computations of Van Vechten and Franck [10] in the case of convection induced by small horizontal temperature gradients in inhomogeneous binary mixtures. So, except for experiments performed in microgravity conditions [11], we think that no reliable measurement of Soret effect may be carried out without the two following conditions being fulfilled:

(1) The hydrodynamical stability diagram of the liquid mixture must be precisely known in order to avoid any departure from the diffusive state.

(2) A continuous control of the hydrodynamical stability must be performed during the Soret measurement in order to prevent any local emergence of nondiffusive motion in the fluid.

In this paper, we shall demonstrate that the use of a convenient technique and the choice of a relevant liquid system makes pure Soret effect measurements possible, free from any convective disturbance.

The remainder of the paper is organized as follows. The scientific goals and technical solutions are developed in Sec. II. The experimental device and procedure are described in Sec. III. Section IV concerns the hydrodynamical study of the system. Section V contains the transport measurement results and a discussion and Sec. VI is a conclusion.

## II. THERMAL DIFFUSION AND CONVECTION MEASUREMENTS IN (LiCl, $RH_2O$) BY HOLOINTERFEROMETRY

The first problem is the selection of the measurement and observation technique. Laser velocimetry enables threshold determination [12], whereas Rayleigh interferometry permits Soret coefficient measurement [13]. But none of these optical methods, given as examples, permits one to perform both studies during the same experiment and check the homogeneity of the two phenomena (diffusion and convection) in the whole working cell. In comparison, holographic interferometry is a powerful optical technique that gives one the opportunity to probe temperature and concentration in the fluid and perform in the same time a continuous and overall visualization of the flow regime of the fluid. This observation of the macroscopic behavior of the liquid permits one to readily identify the instability thresholds and convection regimes. Therefore we intend to investigate the stability diagram in order to highlight the influence of the concentration gradient and determine the conditions for which Soret experiments are not disturbed by the rise of convection. In order to increase the critical temperature difference and therefore the strength of the effect, we have chosen a confined geometry. Consequently we are working in the little-known low aspect ratio domain (height:width: length ratio 3:1:1), unlike the major part of the existing studies, which concern the Rayleigh-Bénard (RB) geometry (only vertical confinement) [4]. Hence we will point out the influence of the confinement on the marginal stability curves and on the convection patterns.

The second problem lies in the choice of a relevant diffusing system. For any class of liquid, no coherent model of the thermal diffusion exists yet [14]. So unlike most of the

 

authors, we have chosen a concentrated aqueous electrolyte (LiCl, $RH_2O$), which brings two advantages. First, numerous measurements of the structure and transport properties of this system at high concentration ($R<12$) are available (see, for example, Refs. [15,16]), whereas the knowledge of its structure is poor at higher dilution. These data will guide a further interpretation of the evolution of the phenomenon with temperature or concentration, which can be regarded as a consequence of the changes in $Li^+$ and $Cl^-$ hydration spheres. Secondly, this system exhibits a structural relaxation that leads to a drastic increase of the viscosity with decreasing temperature. This ensures hydrodynamical stability for high temperature differences (up to 20 °C), yielding significative enrichments. Furthermore, most of the Soret coefficient determinations for aqueous systems deal with low concentrations and temperatures close to ambient [3], which are very peculiar conditions (large hydration of the solute, small range of thermal energy). The understanding of the phenomenon needs the enhancement of the range of experimental values. Hence, our apparatus permits one to cover the low temperatures domain.

## III. EXPERIMENTAL DEVICE

### A. Apparatus

(LiCl, $H_2O$) salt is dried several days at 110 °C then mixed with deionized water. This solution is confined by a rectangular cell of interior dimensions 30 mm (diffusion height)×10 mm (optical path length)×10 mm. The cell is an open parallelepiped made of fused silica with its ends cemented by two unexpandable metal pieces (invar). It is inserted in the cryostatic device shown in Fig. 1. At the top and bottom of the measurement cell, the cold source is a liquid air circulation regulated by an air compressor, and the heat source is a heating electrical wire controlled by a regulator. The temperature ranges from −100 to 40 °C and the temperature difference between top and bottom from 0 to 40 °C. The temperature stability (during several weeks) as well as the measurement accuracy are 0.1 °C. Thermal exchange, air convection, and moisture condensation are minimized by setting the apparatus in a vacuum chamber, which is integrated in the real-time holographic interferometry device.

This device is designed as follows (see Fig. 2). The beam of an argon laser is split into a reference beam and an object beam by a 50/50 beam splitter. The two beams cross a Glan-Taylor prism (vertically polarizing) and a half-wave plate, which gives the opportunity to control their intensity by modifying the polarization direction of the plate. They are both expanded and collimated by a microscope objective-spatial filter-convergent lens set. A parallel plate installed on a rotating mount is inserted between the spatial filter and the convergent lens of the reference beam, which allows us to get rid of parasitic fringes on the initial interferogram. The two beams interfere on the holographic plate, their polarization vectors being parallel and collinear to the plate. The entire setup is enclosed in a plexiglass cover, which permits one to avoid thermal perturbations, and located on a vibrationproof structure [17].

The main interest of holography is the possibility of recording phase objects. The intensity of the interference pattern of the object and reference beams is linked to the phase

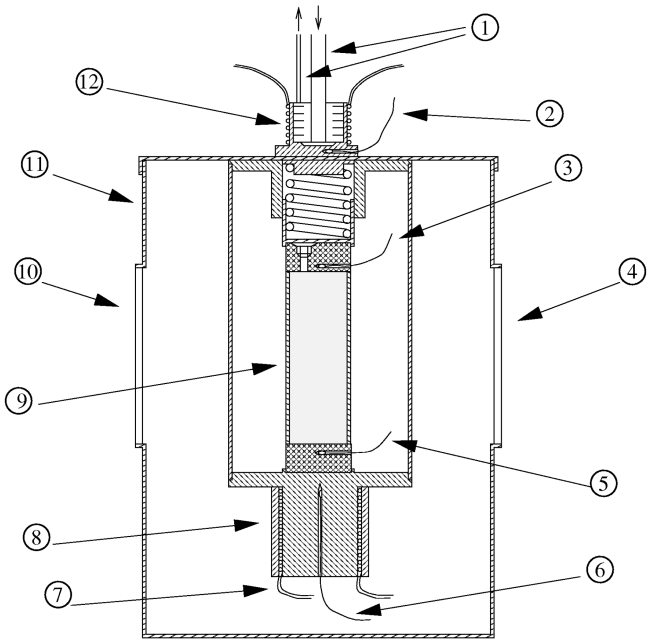


FIG. 1. Experimental cell: (1): Liquid air circulation; (2) and (6): Pt100 probes for high and low regulation temperatures; (3) and (5): Pt100 probes for high and low measurement temperatures; (7) and (12): high and low heating electrical wires; (8) and (11): inner and outer copper heat shields; (9): measurement cell; (4) and (10): optical windows.

of the object beam. In this way, the 3D state of the system at time $t=0$ is recorded on the reference hologram. So our device amounts to a classical interferometer, provided we consider that the reference system is registered on the reference hologram instead of physically existing. In other words, it deals with objects separated in time instead of objects separated in space, which is much more interesting for diffusion studies. The interferograms are visualized and recorded by the use of a video system [charge-coupled device (CCD) camera, microcomputer, monitor, printer, videotape recorder].

So temperature and concentration variations of the fluid, inducing refraction index modifications, are visualized through interference fringes. Lighting durations are limited to a few seconds, thus preventing any local heating of the liquid.

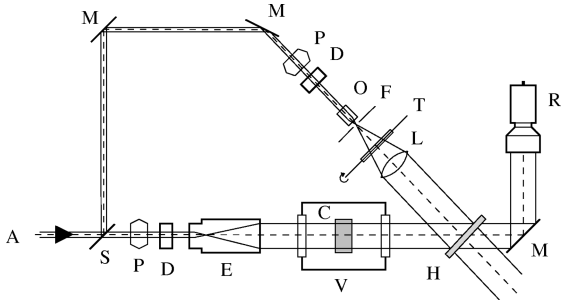


FIG. 2. Holographic setup: (A) Laser beam, (C) experimental cell, (D) half-wave plate, (E) beam expander, (F) spatial filter, (H) holographic plate, (L) convergent lens, (M) mirror, (O) microscope objective, (P) Glan-Taylor prism, (R) video recording system, (S) beam splitter, (T) parallel plate on a rotating mount, and (V) vacuum chamber.

### B. Procedure

The characteristic time $\tau$ of the thermal diffusion is bound to the strength of the interdiffusion (interdiffusion coefficient $D$) and to the diffusion length $h$ [18]:

$$\tau = \frac{h^2}{\pi^2 D}. \tag{1}$$

Similarly, the temperature relaxation time is driven through the same relation by the thermal diffusivity $D_T$. The ratio $\mathrm{Le} = D/D_T$ (Lewis number) is always small in liquids, particularly in our system where $D = 7.7\times10^{-10}$ $\mathrm{m^2\,s^{-1}}$ and $D_T = 1.4\times10^{-7}$ $\mathrm{m^2\,s^{-1}}$, which lead to $\mathrm{Le} = 5.5\times10^{-3}$ at 0 °C. Thanks to this time scale difference, the distinction between thermal and solutal fringes is possible. Once the vertical temperature gradient is settled, the number of appearing fringes is driven by the transient regime of temperature and reaches a steady state in less than half an hour. Subsequently, the first of the concentration fringes appears only after about half a day, achieving the Soret steady state in one to four weeks. This opportunity to distinguish temperature and concentration effects enables us to perform the following procedure:

(1) In the homogeneous mixture, the convection threshold and regime are explored after the recording of a reference hologram at $\Delta T = 0$ by progressively increasing $\Delta T$, keeping the upper end of the cell at constant temperature and increasing the temperature of the lower end. Because the hydrodynamical study lasts a few hours, we can regard the mixture as remaining homogeneous.

(2) We then choose and keep a constant $\Delta T$ for which we have the insurance the liquid is at rest. After making a new reference hologram, we follow the evolution of concentration fringes due to the thermal diffusion.

(3) Once the steady state is nearly attained, a new reference hologram is recorded and a new hydrodynamical study is performed in the same way as in the first phase. Considering that the $\Delta c$ stemming from the diffusion remains constant during this study, we can thereby investigate the influence of this solutal inhomogeneity on the convection thresholds and patterns.

This procedure permits one to perform the physical and dynamical measurements under the same experimental conditions, which is otherwise never the case.

### C. Data analysis

The recording of the interfringe number $N(t)$ during the diffusion (after the second reference hologram) yields the evolution of the weight concentration difference between the hot and cold walls:

$$\Delta c(t) = \frac{N(t)\lambda}{(e\,\partial n/\partial c)}, \tag{2}$$

where $\lambda$ is the laser wavelength ($\lambda = 514$ nm), $e$ the cell optical path length, and $\partial n/\partial c$ the weight concentration derivative of the refraction index. Figure 3 shows an example of the evolution of the concentration interference fringes as a function of time during the thermal diffusion and Fig. 4 displays the corresponding exponential increase of $\Delta c$. After a noise reduction with a low-pass filter, the recording is subsequently fit with Bierlein's equation [18]

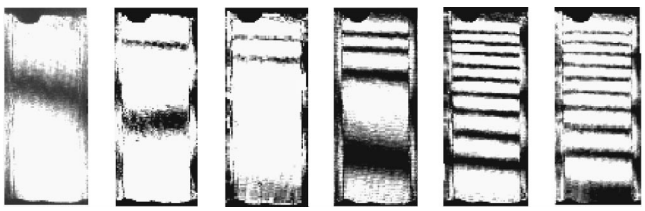

FIG. 3. Evolution of the concentration fringes during a thermal diffusion experiment in a (LiCl, $9.7H_2O$) mixture for $T_{\mathrm{cold}} = -26.5$ °C and $\Delta T = 6.0$ °C from $t = 0$ to $t = 202$ h.

$$\Delta c(t) = \Delta c_\infty \left[1 - \frac{8}{\pi^2} e^{-t/\tau}\right], \tag{3}$$

valid for $t > \tau/2$, from which

$$D = \frac{h^2}{\pi^2 \tau} \quad \text{and} \quad S_T = \frac{1}{c(1-c)} \frac{\Delta c_\infty}{\Delta T} \tag{4}$$

are computed, $c$ being the initial weight concentration of the solute.

The sign of $S_T$ is determined by considering the respective influence of the increase in $\Delta T$ and $\Delta c$ on the optical and mechanical behavior of the liquid. If both increases have similar effects on the system — appearing or destroying of fringes from the optical standpoint, stabilization or unstabilization from the mechanical standpoint — it can be assessed that the denser component migrates towards the cold wall, which corresponds to $S_T > 0$. In the opposite case, $S_T < 0$.

The stability of the system is evaluated by the dimensionless temperature difference $\Delta T$ — thermal Rayleigh number $\mathrm{Ra}_t$ — and the dimensionless concentration difference $\Delta c$ — solute Rayleigh number $\mathrm{Ra}_s$ — defined by

$$\mathrm{Ra}_t = \frac{\alpha g h^3 \Delta T}{\nu D_T} \quad \text{and} \quad \mathrm{Ra}_s = \frac{\beta g h^3 \Delta c}{\nu D}. \tag{5}$$

Here, $\alpha$ and $\beta$ are the dependence coefficients of the density on temperature and concentration, $g$ is the acceleration due

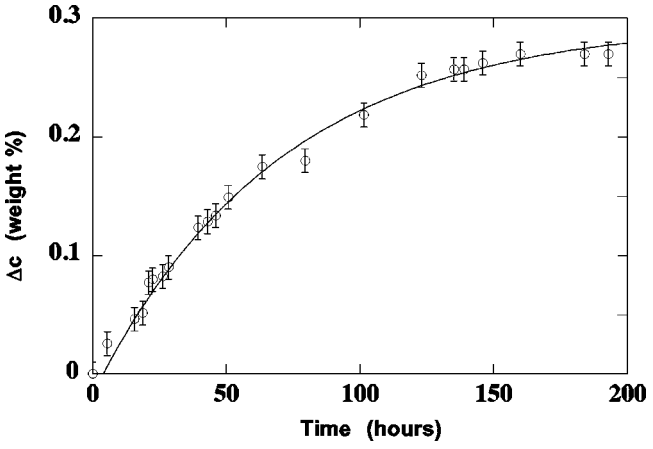


FIG. 4. Concentration difference of LiCl between the hot and cold walls as a function of time for the experiment of Fig. 3.

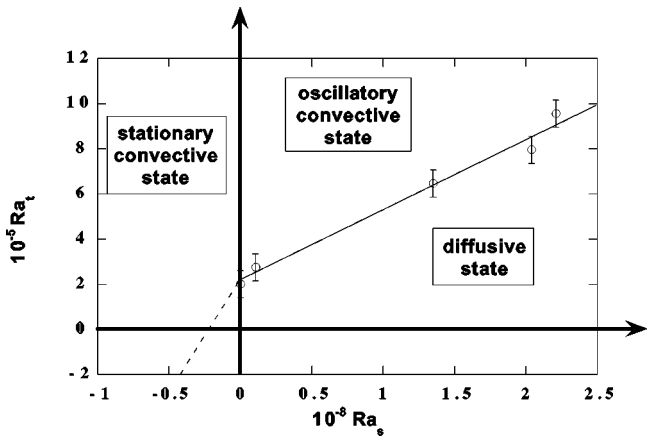


FIG. 5. Critical thermal Rayleigh number $Ra_t$ as a function of the solute Rayleigh number $Ra_s$ of (LiCl, $9.7H_2O$) in a 3:1:1 geometry. The $Ra_s=0$ point corresponds to the homogeneous mixture.

to gravity, $h$ the diffusion length (height of the cell) and $\nu$ the kinematic viscosity. Conventionally, $Ra_t$ is positive when heating from below and $Ra_s$ is positive when the denser component migrates downwards.

## IV. HYDRODYNAMICAL BEHAVIOR OF A CONFINED INHOMOGENEOUS BINARY MIXTURE

In our experimental conditions, unlike in the major part of Soret convection studies, we consider that $\Delta T$ variations do not affect the cell concentration, due to the difference in their time constants. Therefore the stability diagram is drawn in the $(Ra_s, Ra_t)$ plane. Since the system has revealed itself as exhibiting a negative Soret coefficient (see below), we have investigated the $(Ra_s>0,\ Ra_t>0)$ quadrant of the diagram, i.e., heating from below, which provides the most stabilizing and fascinating configuration: the marginal stability curve of the first unstable mode in (LiCl, $9.7H_2O$) is displayed in Fig. 5. The boundary conditions for the ends (invar pieces) are rigid, conducting, and impermeable and the lateral walls (fused silica cell) are conducting compared to the fluid.

The homogeneous mixture behaves like a pure liquid and the first bifurcation leads to a steady convection regime. In our 3:1:1 geometry, it consists of a single roll, the axis of which is randomly (due to the square section) parallel or perpendicular to the interferogram plane (cf. Fig. 6).

As soon as a concentration difference appears in the fluid ($Ra_s>0$, the salt concentrating in the lower part of the cell), the fluid undergoes a Hopf bifurcation as its first instability threshold. Hence oscillations set in, which consist here in a roll, the direction of which periodically changes as shown in Fig. 7.

Very few experimental studies of confined situations have been performed so far. A comparison with the well-studied semi-infinite case — where the oscillatory convective regime leads to the amazing pattern of traveling waves [4]— emphasizes the analogy between the two geometries. However, several features differentiate our configuration from the RB case.

First, the restricted geometry tends to stabilize the liquid with impeding the emergence of motion. The critical $Ra_t$ are therefore high compared to the 1708 of the semi-infinite pure fluid case.

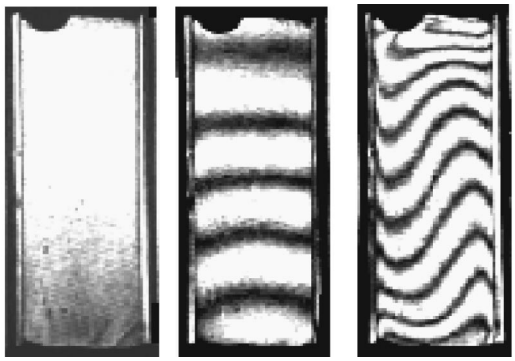

FIG. 6. Evolution of the isotherm's morphology with $\Delta T$ in homogeneous (LiCl, $9.7H_2O$) for a 3:1:1 geometry: stationary convection ($T_{\rm cold}=-38.5$ °C, $\Delta c=0$, and $\Delta T=0.0$ °C$\rightarrow$9.7$\rightarrow$15.5).

Secondly, we have not been able to overturn the periodical behavior of the convection even after increasing $Ra_t$ up to 1.5 $Ra_t^{\rm crit}$, whereas this oscillatory state is always followed by a steady bifurcation in the experimental conditions of standard experiments. This lack of steady overturning convection can be attributed to three factors. First, according to the computations of Barten *et al.* [19], the small value of the Lewis number could account for a large oscillatory domain, delaying the second transition to large $Ra_t$. Then, the greatness of the $Ra_s$ values also supports this lack (see, for instance, [20]). Finally, unlike Moses and Steinberg in a $Ra_s<0$ case [21] and like Liu and de Bruyn in a $Ra_s>0$ case [22], we think that the trend of the confinement is to reinforce the stability of the oscillatory state. But further experiments are needed to distinguish the respective influence of each factor.

Thirdly, like Liu and de Bruyn [22], we find that the restricted environment enhances the influence of the concentration. Unlike the semi-infinite case, where the oscillatory threshold is very insensitive to the magnitude of the solutal inhomogeneity, the slope of $Ra_t^{\rm crit}$ against $Ra_s$ is very large in our case.

What is still difficult to state is the criticality of the phenomenon. In the extended geometry, the larger $Ra_s$, the more undercritical the bifurcation is [4]. We experience a gap in the amplitude of the isotherms distortion at onset, and the oscillations are reached via a hysteretic transition. But

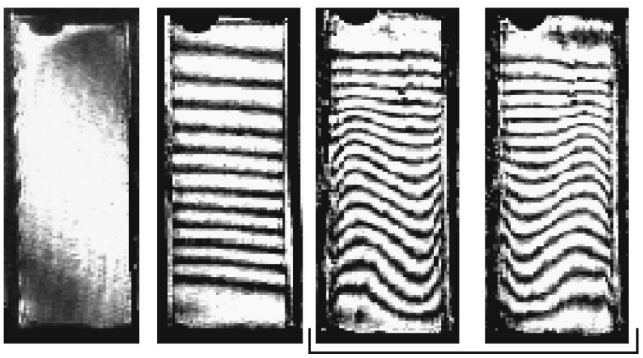

FIG. 7. Evolution of the isotherm's morphology with $\Delta T$ in inhomogeneous (LiCl, $9.7H_2O$) for a 3:1:1 geometry: oscillatory convection, the roll changes direction with a period $t=72$ s ($T_{\rm cold}=-38.5$ °C, $\Delta c=0.32$ wt % and $\Delta T=0.0$ °C$\rightarrow$25.1$\rightarrow$31.0).

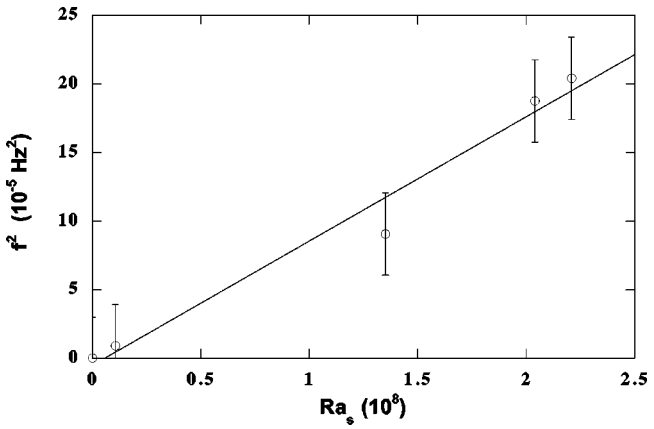


FIG. 8. Frequency measured at the onset of oscillations in (LiCl, $9.7H_2O$) as a function of $Ra_s$ in the 3:1:1 geometry.

these facts can be accounted for by the undercriticality of the phenomenon as much as by experimental inertia.

Finally, in the Rayleigh-Bénard experiments, the evolution of the frequency of the marginal oscillations $f$ can be theoretically predicted, using a linear stability analysis with the unrealistic conditions of free boundaries, as following a $\sqrt{Ra_s - Ra_t}$ law [23]. The very low value of our Lewis number implies that $Ra_t$ is very small compared to $Ra_s$. Keeping this in mind, we have made the following acknowledgments: near onset, $f$ is independant of $Ra_t$ and $f^2$ at onset is a linear function of $Ra_s$ as plotted in Fig. 8. So, despite the crude approximation of the model, the trend of the theoretical relation is still valid in a confined geometry.

Once the discovery of the hydrodynamical behavior of the liquid mixture in our experimental conditions is achieved, we can be confident in our transport measurements. Provided the overall stability of the liquid is controlled during the entire thermal diffusion (to detect eventual local motions), choosing a $\Delta T$ value in the diffusive domain will keep us from meeting the cumbersome effect of convection.

## V. TRANSPORT PROPERTIES OF (LiCl, $9.7H_2O$)

We have investigated the interdiffusion and Soret coefficients variations with temperature for a (LiCl, $9.7H_2O$) mixture.

In spite of the abundant literature concerning self- and interdiffusion of aqueous lithium chloride, no measurements at low temperature exist yet. So Soret experiments reveal themselves to be an original method for measuring other solutal transport coefficients.

Figure 9 displays, on an Arrhenian plot, our interdiffusion coefficient values as well as the literature ones for the same concentration around room temperature [24]. (LiCl, $9.7H_2O$) being a fragile glass, according to Angell's classification [25], its structural relaxation cannot be described by a single thermally activated process (of activation energy $\Delta E_D$). So we can verify that the evolution of $D$ with $T$ does not follow an Arrhenius law

$$D = D_0 T \exp\frac{\Delta E_D}{kT} \tag{6}$$

when approaching the liquidus temperature.

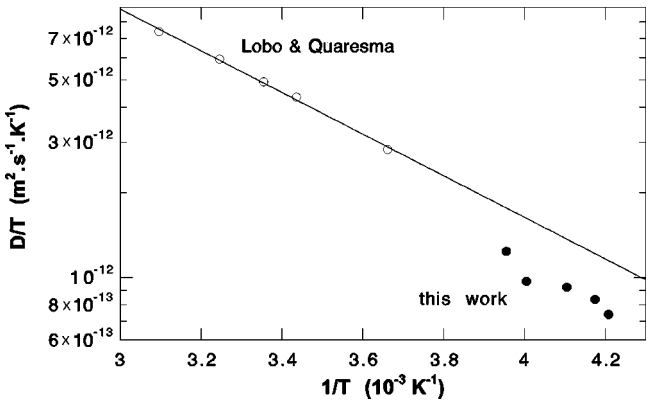


FIG. 9. $\ln(D/T)$ of (LiCl, $9.7H_2O$) as a function of $1/T$, including literature results [24].

The Stokes-Einstein law

$$D = A\frac{kT}{r\eta} \tag{7}$$

is based on a hydrodynamical model of diffusion, which considers ions as spheres of radius $r$ migrating in a continuous medium characterized by its viscosity $\eta$. In concentrated mixtures, the prefactor $A$, related to geometric considerations, is not precisely known owing to the ion-ion interactions. So we have calculated $A$ from a fit of the literature results and we can check in Fig. 10 the agreement of our low temperature values with the ambient temperature ones.

The Soret coefficient of (LiCl, $9.7H_2O$) as a function of temperature is displayed in Fig. 11. Always negative, it exhibits a slow increase in temperature. In the literature, the only Soret effect experiments as a function of the temperature of this system are Wood and Hawksworth's conductimetric measurements (0.01 mol/l, i.e., $R = 5550$) [26] and Alexander's thermogravitational column results (0.05 mol/l, i.e., $R = 1110$) [27]: $S_T$ also shows a gentle rise, changing sign from negative to positive as shown in Fig. 11. Two inferences may be drawn from these experiments:

(1) The intensity of the thermal diffusion grows when the concentration is enhanced. Increasing the concentration leads

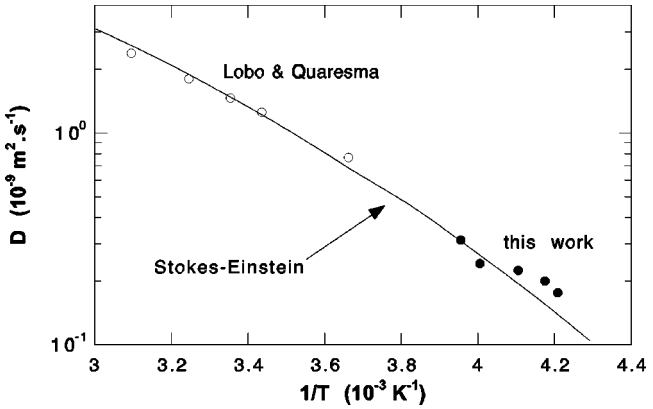


FIG. 10. $\ln D$ of (LiCl, $9.7H_2O$) as a function of $1/T$, including literature results [24] and a prediction of the evolution of $D$ towards cold temperatures based on a Stokes-Einstein law.

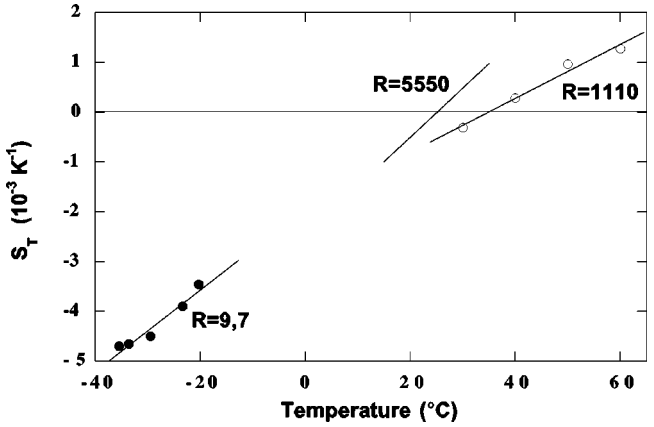


FIG. 11. Soret coefficient of (LiCl, $RH_2O$) as a function of the temperature. The $R=5550$ results are from [26] and the $R=1110$ are from [27]. The experimental values are fitted linearly.

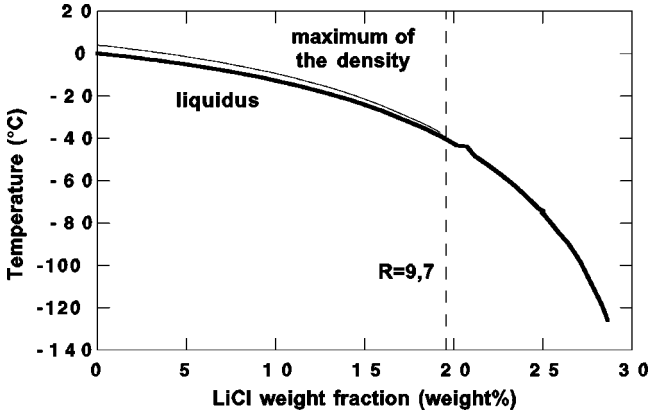


FIG. 12. Phase diagram of (LiCl, $H_2O$) [29], including the values of the maximum of the density [28].

at a microscopic scale to a decay of the volume of influence of each ion on water, being reduced at $R=6$ to one hydration sphere [16]. In dilute salt solutions, the tetrahedral structure of water prevails, because the abundance of free water (not bound to ions) enables a high number of H bonds per water molecules. In concentrated salt solutions, this glasslike structure has nearly disappeared because all the water molecules are polarized by the Coulombic atmosphere of the ions and adopt its spherical organization. At first glance, the ionic organization is more favorable to demixion in the system.

(2) Lin attempts to explain this Soret coefficient sign inversion by considering the change of sign of $(\partial\rho/\partial T)_{P,c}$ in such solutions [14], the density exhibiting a maximum in this temperature range (4 °C for pure water). Indeed, during the diffusion, a moving particle causes a local rise of pressure ahead, leading to an increase of the density. Depending on the sign of $(\partial\rho/\partial T)_{P,c}$, it gives rise to a decrease or an increase of the temperature, provoking a migration of the particule toward the hot or cold wall. But we know that the temperature of the maximum of the density decays with increasing concentration, in a parallel way with the liquidus, following the law [28]

$$T_m(X)=\left(1.0147-2.67\times10^{-2}\frac{X}{1-X}\right)T_l(X), \qquad (8)$$

with $X=x/(1-6x)$, $x$ molar fraction of LiCl, and $T_l$ temperature of the liquidus, as displayed in Fig. 12. So our measurements are inconsistent with Lin's prediction because $S_T$ of the $R=9.7$ mixture is far from exhibiting a sign inversion at $T_m=-38$ °C. So we can assume that temperature changes due to compression-expansion are not the only contribution to the Soret effect, especially for high concentrations.

These two assumptions need further experiments with different concentration and temperature ranges in order to find all the significant mechanisms contributing to the Soret effect.

## VI. CONCLUSION

In conclusion, we have presented a study that combines an original experimental technique — holographic interferometry — and a little-studied system — concentrated aqueous LiCl. It permits one on one hand to fully investigate the hydrodynamical behavior of the confined mixture. We have compared our stability diagram and convective patterns with the Rayleigh-Bénard geometry. Agreement is good but some questions still have to be clarified such as the lack of steady overturning convection and the criticality of the bifurcation. On the other hand, this dynamical study has enabled us to measure a pure Soret effect, free from any convective disturbance. Comparison with literature results in other conditions has led to contradict a possible explanation of the evolution of the Soret coefficient with temperature. But more experiments are needed to highlight the effect of ionic and molecular structure on this transport property.

## ACKNOWLEDGMENTS

This research is supported by the Centre National d'Etudes Spatiales (France). We would like to thank Daniel Henry for stimulating discussions, and Ludovic Bellon and Sébastien Chaumat for their experimental help.

[1] B. Rousseau, A. Fuchs, and J. Simon, Entropie **184/185**, 62 (1994).
[2] W. Köhler, J. Chem. Phys. **98**, 660 (1993).
[3] T. Griffiths and N. Phillips, J. Electrochem. Soc. **138**, 3575 (1991).
[4] M. Cross and P. Hohenberg, Rev. Mod. Phys. **65**, 998 (1993).
[5] J. Legros, P. Goemaere, and J. Platten, Phys. Rev. A **32**, 1903 (1985).
[6] P. Kolodner, H. Williams, and C. Moe, J. Chem. Phys. **88**, 6512 (1988).
[7] O. Ecenarro *et al.*, J. Phys.: Condens. Matter **2**, 2289 (1990).
[8] W. Köhler and B. Müller, J. Chem. Phys. **103**, 4367 (1995).

[9] K. Zhang, M. Briggs, R. Gammon, and J. Sengers, J. Chem. Phys. **104**, 6881 (1996).
[10] T. Van Vechten and C. Franck, Phys. Rev. E **48**, 3635 (1993).
[11] J. Bert and J. Dupuy-Philon, J. Phys.: Condens. Matter **9**, 11 045 (1997).
[12] O. Lhost and J. Platten, Phys. Rev. A **38**, 3147 (1988).
[13] L. Longsworth, J. Phys. Chem. **61**, 1557 (1957).
[14] J. Lin, W. Taylor, W. Rutherford, and J. Millat, in *Measurement of the Transport Properties of Fluids*, edited by W. A. Wakehan, A. Nagashima, and J. V. Sengers (Blackwell Scientific, Oxford, 1991), p. 321.
[15] B. Prével, J. Jal, J. Dupuy-Philon, and A. Soper, J. Chem. Phys. **103**, 1886 (1995).
[16] J. Jal, A. Soper, P. Carmona, and J. Dupuy, J. Phys.: Condens. Matter **3**, 551 (1991).
[17] H. Dez, Ph.D. thesis, Lyon, 1992.
[18] J. Bierlein, J. Chem. Phys. **23**, 10 (1955).
[19] W. Barten, M. Lücke, M. Kamps, and R. Schmitz, Phys. Rev. E **51**, 5636 (1995).
[20] H. Touiri, J. Platten, and G. Chavepeyer, Eur. J. Mech. B/ Fluids **15**, 241 (1996).
[21] E. Moses and V. Steinberg, Phys. Rev. A **43**, 707 (1991).
[22] M. Liu and J. de Bruyn, Can. J. Phys. **70**, 689 (1992).
[23] J. Platten and J. Legros, in *Convection in Liquids* (Springer-Verlag, Berlin, 1984), p. 566.
[24] V. Lobo and J. Quaresma, in *Physical Sciences Data 41, Handbook of Electrolyte Solutions, Part B* (Elsevier, Amsterdam, 1989), pp. 1200–1201.
[25] C. Angell, J. Non-Cryst. Solids **131-133**, 13 (1991).
[26] C. Wood and W. Hawksworth, J. S. Afr. Chem. Inst. **24**, 170 (1971).
[27] K. Alexander, Z. Phys. Chem. (Leipzig) **203**, 213 (1954).
[28] A. El Hachadi, Ph.D. thesis, Lyon, 1991.
[29] R. Cohen-Adad and J. Lorimer, *Solubility Data Series, Alkali Metal and Ammonium Chlorides in Water and Heavy Water (binary systems)* (Pergamon Press, Oxford, 1991), Vol. 47.